

# The dynamics of free, straight dislocation pairs. II. Edge dislocations

R. Eykholt

*Department of Physics, Colorado State University, Fort Collins, Colorado 80523 and Los Alamos National Laboratory, Los Alamos, New Mexico 87545*

D. J. Srolovitz

*Department of Materials Science and Engineering, University of Michigan, Ann Arbor, Michigan 48109-2136 and Los Alamos National Laboratory, Los Alamos, New Mexico 87545*

(Received 31 October 1988; accepted for publication 1 February 1989)

We present a detailed analysis of the relative motion of a pair of edge dislocations with parallel line directions due to their mutual interactions in the overdamped limit. In particular, we derive analytic expressions for the trajectories in the three cases of parallel, antiparallel, and perpendicular Burgers vectors for both zero climb and finite climb. In each of these cases, we find attracting (stable) or repelling (unstable) equilibria, and this allows a simple characterization of the motion. For all other orientations, no such equilibria exist, and the two dislocations either come together or escape to infinity. In addition, we give the equations of motion for the trajectories in the presence of an external stress.

## I. INTRODUCTION

In a previous paper<sup>1</sup> (hereafter referred to as I), the present authors have analyzed the motion of a pair of interacting, straight screw dislocations. The trajectories of both parallel and antiparallel pairs of screw dislocations were determined as a function of the applied stress, the damping factor (e.g., due to phonon radiation), the effective mass of the dislocations, and the elastic constants of the material. These results were then employed in a simple statistical analysis of systems with many dislocations. The present paper extends the results of I to the more interesting (and more complex) case of pairs of edge dislocations.

Our overall interest in dislocation dynamics is in describing the plastic properties of the dynamics of the interacting defects which carry the deformation. Although this objective is indeed ambitious, we view the present study as a first step in that direction. The next jump to be made is the extension of the present two-dislocation analysis to an analysis of the dynamics of a large number of interesting dislocations. However, the complexity of accounting for more than two dislocations is formidable, and numerical analyses/simulations will be required. Some preliminary results from both cellular-automaton<sup>2</sup> and molecular-dynamics simulations of systems containing many dislocations are available.<sup>3,4</sup> Unfortunately, these simulations are usually unable to use the experimental values of both the dislocation densities and the time scales. This problem can be alleviated, in part, by the incorporation of a knowledge of the trajectories of pairs of dislocations. These trajectories can be used to avoid the extremely small time steps which are necessary to account for the motion of dislocations that are very close together.

In the present paper, we derive analytic expressions for the motion of pairs of edge dislocations in two spatial dimensions (i.e., straight dislocations with parallel line directions). We assume that the system is infinite in extent, and we neglect any Peierls stress. The general equations of motion for pairs of edge dislocations are discussed in Sec. II.

Section III describes a "center-of-mass" coordinate system. Pairs of dislocations with parallel, antiparallel, and perpendicular Burgers vectors are considered in Secs. IV, V, and VI, respectively. Finally, the case of dislocations with arbitrary Burgers vectors is discussed. In general, the edge-dislocation results are less complete than for pairs of screw dislocations (see I) due to the added complexity of their anisotropic interactions and mobilities. Nevertheless, a number of interesting and useful results are obtained.

## II. EQUATIONS OF MOTION

We consider two parallel edge dislocations with effective mass  $m^*$  (Ref. 5) and Burgers vectors  $\mathbf{b}_1$  and  $\mathbf{b}_2$  of equal magnitude  $b$  in the presence of an external stress  $\boldsymbol{\sigma}$ . We choose a coordinate system with its  $z$  axis parallel to the line direction of the dislocations and its  $x$  axis along  $\mathbf{b}_1$ , we let  $\alpha$  denote the angle between the Burgers vectors (choosing our labeling so that  $0 \leq \alpha < \pi$ ), and we denote the positions of the dislocations by vectors  $\mathbf{r}_1$  and  $\mathbf{r}_2$  in the  $xy$  plane, with  $\mathbf{r} = \mathbf{r}_1 - \mathbf{r}_2$  denoting their relative separation. For convenience, we also consider a  $\xi\eta$  coordinate system rotated by  $\alpha$ , so that the  $\xi$  axis is along  $\mathbf{b}_2$  (see Fig. 1).

The interaction potential between these two dislocations is<sup>6</sup>

$$\begin{aligned} V(\mathbf{r}) &= \frac{\mu}{2\pi(1-\nu)} \left[ (\mathbf{b}_1 \cdot \mathbf{b}_2) \left( \ln \frac{R_c}{r} - \frac{3}{2} \right) \right. \\ &\quad \left. + \frac{(\mathbf{b}_1 \cdot \mathbf{r})(\mathbf{b}_2 \cdot \mathbf{r})}{r^2} \right] \\ &= \frac{\mu b^2}{2\pi(1-\nu)} \left[ \left( \ln \frac{R_c}{r} - \frac{3}{2} \right) \cos \alpha \right. \\ &\quad \left. + \cos \theta \cos(\theta - \alpha) \right], \end{aligned} \quad (1)$$

where  $\mu$  is the shear modulus,  $\nu$  is the Poisson ratio,  $\theta$  is the polar angle of  $\mathbf{r}$ , and  $R_c$  is the outer cutoff distance. Differentiation of Eq. (1) with respect to the dislocation coordinates yields the forces on dislocation 1 due to dislocation 2 ( $\mathbf{f}_1$ )

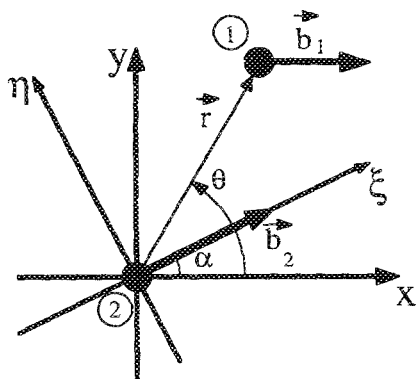


FIG. 1. Illustration of the coordinate systems employed. For the  $xy$  system, the  $x$  axis is placed along the Burgers vector  $b_1$ , and for the  $\xi\eta$  system, the  $\xi$  axis is placed along the Burgers vector  $b_2$ . Since we will be dealing mainly with the relative motion  $r = r_1 - r_2$ , dislocation 2 has been placed at the origin.

and on dislocation 2 due to dislocation 1 ( $f_2$ ):

$$f_1 = \frac{\mu b^2}{2\pi(1-\nu)r} \{ \hat{x} \cos 2\theta \cos(\theta - \alpha) + \hat{y} [\sin(\theta - \alpha) + \sin 2\theta \cos(\theta - \alpha)] \}, \quad (2)$$

$$f_2 = -\frac{\mu b^2}{2\pi(1-\nu)r} \{ \hat{\xi} \cos \theta \cos 2(\theta - \alpha) + \hat{\eta} [\sin \theta + \cos \theta \sin 2(\theta - \alpha)] \}, \quad (3)$$

where a caret ( $\hat{\phantom{x}}$ ) indicates a unit vector. In addition, an externally applied stress creates forces on the dislocations which may be determined through the Peach-Koehler formula<sup>7</sup>

$$F = (b \cdot \sigma) \times \hat{z}, \quad (4)$$

leading to the forces (letting  $F_{ij} = b\sigma_{ij}$ )

$$F_1 = \hat{x}F_{xy} - \hat{y}F_{xx}, \quad (5)$$

$$F_2 = \hat{\xi} [F_{xy} \cos 2\alpha + (F_{yy} - F_{xx}) \sin \alpha \cos \alpha] - \hat{\eta} (F_{xy} \sin 2\alpha + F_{xx} \cos^2 \alpha + F_{yy} \sin^2 \alpha). \quad (6)$$

Since all of these calculations are performed within the framework of linear elasticity, the interaction forces [Eqs. (2) and (3)] and those due to the applied stress [Eqs. (5) and (6)] may simply be added.

In order to relate the force on a dislocation to its subsequent motion, we need to consider how a dislocation moves through a material. For motion through a crystalline lattice, there is movement of both the atoms in the core region of the dislocation and those far away. The faster the dislocation moves, the more kinetic energy is imparted to these atoms. Neglecting the relatively small contribution of the dislocation core, this kinetic energy scales as the square of the dislocation velocity.<sup>5,8</sup> Therefore, the dislocation has an effective mass  $m^*$ , which is given by<sup>5,8</sup>

$$E_{\text{kin}} = \frac{1}{2} m^* v^2 = \frac{\mu b^2}{8\pi(1-\nu)} \frac{v^2}{c^2} \ln\left(\frac{R_c}{r_c}\right) \quad (7)$$

or

$$m^* = \frac{\mu b^2}{4\pi(1-\nu)c^2} \ln\left(\frac{R_c}{r_c}\right), \quad (8)$$

where  $c$  is the sound velocity and  $r_c$  is the inner cutoff distance. Since a moving dislocation has mass, it carries momentum, and, hence, should behave as a Newtonian particle:  $m^* \ddot{x} = F$ , where the dots indicate differentiation with respect to time, and  $F$  is the force on the dislocation.

Since dislocations in metals exist on a lattice, instead of in a true continuum, a moving dislocation radiates phonons. Therefore, the movement of the dislocation dissipates energy, and its motion is nonconservative. In addition to the aforementioned phonon-emission dissipation mechanism, a number of other dissipation mechanisms are known to exist.<sup>8</sup> In metals, the scattering of thermal phonons by the moving dislocation is the dominant dissipation mechanism, except at very low temperatures.<sup>8</sup> This dissipation modifies the equation of motion for the dislocation:

$$F = m^* \ddot{x} + \gamma \dot{x}, \quad (9)$$

where<sup>8</sup>

$$\gamma = \mu b g(T)/c, \quad (10)$$

and where  $g(T)$  is a temperature-dependent numerical constant of order  $10^{-2}$ .

When the dislocation is climbing (i.e., moving in the direction normal to its slip plane), an additional source of damping is present. This additional damping generally dominates all other forms of damping and is related to the diffusion necessary for climb. Thus, for dislocation motion in the direction *normal* to the slip plane, we replace the phonon-scattering damping  $\gamma$  with the diffusion-controlled damping<sup>8</sup>

$$\Gamma \approx D_s \Omega / b^2 kT, \quad (11)$$

where  $D_s$  is the self-diffusion coefficient,  $\Omega$  is an atomic volume, and  $kT$  is the thermal energy. Since the damping is different for dislocation glide and climb, the damping is anisotropic. In most cases,  $\Gamma$  exceeds  $\gamma$  by many orders of magnitude, and, hence, glide is very much faster than climb.

Combining these results for the forces and the dynamics finally yields the four equations of motion (two coordinates for each dislocation):

$$m^* \ddot{x}_1 + \gamma \dot{x}_1 = \frac{\mu b^2}{2\pi(1-\nu)r} \cos 2\theta \cos(\theta - \alpha) + F_{xy}, \quad (12)$$

$$m^* \ddot{y}_1 + \Gamma \dot{y}_1 = \frac{\mu b^2}{2\pi(1-\nu)r} [\sin(\theta - \alpha) + \sin 2\theta \cos(\theta - \alpha)] - F_{xx}, \quad (13)$$

$$m^* \ddot{\xi}_2 + \gamma \dot{\xi}_2 = -\frac{\mu b^2}{2\pi(1-\nu)r} \cos \theta \cos 2(\theta - \alpha) + F_{xy} \cos 2\alpha + (F_{yy} - F_{xx}) \sin \alpha \cos \alpha, \quad (14)$$

$$m^* \ddot{\eta}_2 + \Gamma \dot{\eta}_2 = -\frac{\mu b^2}{2\pi(1-\nu)r} \times [\sin \theta + \cos \theta \sin 2(\theta - \alpha)] - F_{xy} \sin 2\alpha - F_{xx} \cos^2 \alpha - F_{yy} \sin^2 \alpha. \quad (15)$$

Since the damping term usually dominates the inertial term, we will be considering these equations primarily in the over-

damped limit ( $m^* \rightarrow 0$ ), in which case, the first term on the left-hand side of each equation may be dropped.

### III. CENTER-OF-MASS MOTION

Because the interaction potential (1) depends only on the relative coordinate  $\mathbf{r} = \mathbf{r}_1 - \mathbf{r}_2$ , it is useful to change variables from the individual positions  $\mathbf{r}_1$  and  $\mathbf{r}_2$  to the relative and center-of-mass coordinates  $\mathbf{r}$  and  $\mathbf{R}$ . However, due to the anisotropic damping, unless the Burgers vectors are either parallel ( $\alpha = 0$ ) or antiparallel ( $\alpha = \pi$ ), the equation of motion for the center of mass  $\mathbf{R}$  involves the relative coordinate  $\mathbf{r}$ , and, as a result, the center-of-mass motion is neither simple nor particularly illuminating.

To illustrate this point, consider the overdamped limit ( $m^* \rightarrow 0$ ) in the case of zero climb (i.e.,  $\Gamma \rightarrow \infty$ ), and in the absence of external stress ( $F_{ij} = 0$ ), in which case, the equations of motion become

$$\gamma \dot{x}_1 = \frac{\mu b^2}{2\pi(1-\nu)r} \cos 2\theta \cos(\theta - \alpha), \quad (16)$$

$$\gamma \dot{\xi}_2 = -\frac{\mu b^2}{2\pi(1-\nu)r} \cos \theta \cos 2(\theta - \alpha), \quad (17)$$

$$\dot{y}_1 = 0, \quad (18)$$

$$\dot{\eta}_2 = 0. \quad (19)$$

Therefore, the center-of-mass coordinates,

$$X = \frac{1}{2}(x_1 + x_2) = \frac{1}{2}(x_1 + \xi_2 \cos \alpha - \eta_2 \sin \alpha), \quad (20)$$

$$Y = \frac{1}{2}(y_1 + y_2) = \frac{1}{2}(y_1 + \xi_2 \sin \alpha + \eta_2 \cos \alpha), \quad (21)$$

satisfy the equations of motion (after some simplifying algebra),

$$\gamma \dot{X} = -\frac{\mu b^2}{4\pi(1-\nu)r} \sin \alpha [\sin \theta + \cos \theta \sin 2(\theta - \alpha)], \quad (22)$$

$$\gamma \dot{Y} = -\frac{\mu b^2}{4\pi(1-\nu)r} \sin \alpha \cos \theta \cos 2(\theta - \alpha), \quad (23)$$

showing that, even with zero climb, with no inertia, and in the absence of external stress, the center of mass undergoes a complicated motion, unless either  $\alpha = 0$  or  $\alpha = \pi$  (parallel or antiparallel Burgers vectors).

For parallel ( $\epsilon = 1$ ) or antiparallel ( $\epsilon = -1$ ) Burgers vectors, the equations of motion (12)–(15) become

$$m^* \ddot{x}_1 + \gamma \dot{x}_1 = \frac{\epsilon \mu b^2}{2\pi(1-\nu)r} \cos \theta \cos 2\theta + F_{xy}, \quad (24)$$

$$m^* \ddot{y}_1 + \Gamma \dot{y}_1 = \frac{\epsilon \mu b^2}{2\pi(1-\nu)r} \sin \theta (1 + 2 \cos^2 \theta) - F_{xx}, \quad (25)$$

$$m^* \ddot{x}_2 + \gamma \dot{x}_2 = -\frac{\epsilon \mu b^2}{2\pi(1-\nu)r} \cos \theta \cos 2\theta + \epsilon F_{xy}, \quad (26)$$

$$m^* \ddot{y}_2 + \Gamma \dot{y}_2 = -\frac{\epsilon \mu b^2}{2\pi(1-\nu)r} \sin \theta (1 + 2 \cos^2 \theta) - \epsilon F_{xx}. \quad (27)$$

Thus, the center-of-mass coordinates satisfy the equations

$$m^* \ddot{X} + \gamma \dot{X} = [(1 + \epsilon)/2] F_{xy}, \quad (28)$$

$$m^* \ddot{Y} + \Gamma \dot{Y} = -[(1 + \epsilon)/2] F_{xx}, \quad (29)$$

which yield the center-of-mass motion

$$X = X_0 + \frac{1 + \epsilon}{2\gamma} F_{xy} t + \frac{m^*}{\gamma} \left( V_{x0} - \frac{1 + \epsilon}{2\gamma} F_{xy} \right) (1 - e^{-\gamma t/m^*}), \quad (30)$$

$$Y = Y_0 - \frac{1 + \epsilon}{2\Gamma} F_{xx} t + \frac{m^*}{\Gamma} \left( V_{y0} + \frac{1 + \epsilon}{2\Gamma} F_{xx} \right) (1 - e^{-\Gamma t/m^*}). \quad (31)$$

In the overdamped limit ( $m^* \rightarrow 0$ ) with no climb ( $\Gamma \rightarrow \infty$ ), this reduces to

$$X = X_0 + [(1 + \epsilon)/2\gamma] F_{xy} t, \quad (32)$$

$$Y = Y_0. \quad (33)$$

These results illustrate the fact that the effects of the finite effective mass of the dislocations decay away exponentially fast with the two time constants  $\tau_1 = m^*/\gamma$  and  $\tau_2 = m^*/\Gamma \ll \tau_1$ . Inserting experimental data for copper into the expressions for  $m^*$  and  $\gamma$  [Eqs. (8) and (10)], we find that  $\tau_1 \approx 5 \times 10^{-12}$  s. If the dislocation were traveling at the shear-wave velocity, it would decay to its overdamped velocity in a distance of order 10 Å. Since these time constants are so small, we restrict our attention to the overdamped limit for the remainder of this paper.

For completeness, we conclude this section by giving the general equations of motion for the relative coordinate  $\mathbf{r} = \mathbf{r}_1 - \mathbf{r}_2 = (\hat{x}x + \hat{y}y)$  in the overdamped limit:

$$\begin{aligned} \dot{x} = & \frac{\mu b^2}{2\pi\gamma(1-\nu)} (x^2 + y^2)^{-2} [2x(x^2 - y^2)\cos^3 \alpha + x^2y \sin \alpha (1 + 4 \cos^2 \alpha) - y^3 \sin \alpha] \\ & + \frac{\mu b^2 \sin \alpha}{2\pi\Gamma(1-\nu)} (x^2 + y^2)^{-2} [2x(x^2 - y^2)\sin \alpha \cos \alpha + x^2y(1 - 4 \cos^2 \alpha) - y^3] \\ & + F_{xy} \left( \frac{1 - \cos \alpha \cos 2\alpha}{\gamma} - \frac{2 \sin^2 \alpha \cos \alpha}{\Gamma} \right) + F_{xx} \left( \frac{1}{\gamma} - \frac{1}{\Gamma} \right) \sin \alpha \cos^2 \alpha - F_{yy} \sin \alpha \left( \frac{\cos^2 \alpha}{\gamma} + \frac{\sin^2 \alpha}{\Gamma} \right), \quad (34) \end{aligned}$$

$$\begin{aligned} \dot{y} = & \frac{\mu b^2 \sin \alpha}{2\pi\gamma(1-\nu)} x(x^2 + y^2)^{-2} [(x^2 - y^2)\cos 2\alpha + 2xy \sin 2\alpha] \\ & - \frac{\mu b^2}{2\pi\Gamma(1-\nu)} (x^2 + y^2)^{-2} [x(1 + 2 \cos^2 \alpha)(x^2 \sin \alpha - 2xy \cos \alpha - y^2 \sin \alpha) - 2y^3 \cos \alpha] \\ & - F_{xy} \sin \alpha \left( \frac{\cos 2\alpha}{\gamma} - \frac{2 \cos^2 \alpha}{\Gamma} \right) + F_{xx} \left( \frac{\sin^2 \alpha \cos \alpha}{\gamma} - \frac{1 - \cos^3 \alpha}{\Gamma} \right) - F_{yy} \left( \frac{1}{\gamma} - \frac{1}{\Gamma} \right) \sin^2 \alpha \cos \alpha. \quad (35) \end{aligned}$$

Although these equations are easy to solve numerically, they are tractable analytically only for the special cases of parallel ( $\alpha = 0$ ), antiparallel ( $\alpha = \pi$ ), or perpendicular ( $\alpha = \pi/2$ ) Burgers vectors.

#### IV. PARALLEL BURGERS VECTORS ( $\alpha = 0$ )

For  $\alpha = 0$ , the overdamped equations of relative motion (34) and (35) become independent of the external stress:

$$\dot{x} = \frac{\mu b^2 x (x^2 - y^2)}{\pi \gamma (1 - \nu) (x^2 + y^2)^2}, \quad (36)$$

$$\dot{y} = \frac{\mu b^2 y (3x^2 + y^2)}{\pi \Gamma (1 - \nu) (x^2 + y^2)^2}. \quad (37)$$

We begin with the zero-climb limit ( $\Gamma \rightarrow \infty$ ), in which case, the second equation becomes  $\dot{y} = 0$  or  $y = y_0 = y(0)$ . Thus, the first equation now becomes

$$\dot{x} = \frac{\mu b^2 x (x^2 - y_0^2)}{\pi \gamma (1 - \nu) (x^2 + y_0^2)^2}. \quad (38)$$

For  $y_0 = 0$ , this is easily solved to yield [with  $x_0 = x(0)$ ]

$$x = x_0 \left( 1 + \frac{2\mu b^2 t}{\pi \gamma (1 - \nu) x_0^2} \right)^{1/2}, \quad (39)$$

while, for  $y_0 \neq 0$ , it gives

$$t = \frac{\pi \gamma (1 - \nu)}{2\mu b^2} \left[ x^2 - x_0^2 - 2y_0^2 \ln \left( \frac{x}{x_0} \right) + 4y_0^2 \ln \left( \frac{x^2 - y_0^2}{x_0^2 - y_0^2} \right) \right], \quad (40)$$

which cannot be analytically inverted to yield  $x(t)$ .

For  $y_0 = 0$ , the relative motion is along the line  $y = 0$  and away from the point  $x = 0$ , with the asymptotic behavior (as  $t \rightarrow \infty$ )

$$|x| \rightarrow \left( \frac{2\mu b^2 t}{\pi \gamma (1 - \nu)} \right)^{1/2}. \quad (41)$$

For  $y_0 \neq 0$ , the relative motion is along the line  $y = y_0$ , away from the "stagnation" points  $x = \pm y_0$  (where  $\dot{x} = \dot{y} = 0$ ), and toward the values  $x = 0$ , or  $x = \pm \infty$  (as shown in Fig. 2). In this case, the asymptotic behavior is (as  $t \rightarrow \infty$ )

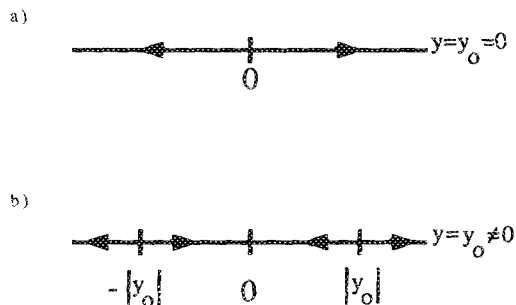


FIG. 2. For parallel Burgers vectors ( $\alpha = 0$ ) in the overdamped limit ( $m^* \rightarrow 0$ ) with zero climb ( $\Gamma \rightarrow \infty$ ), the  $y$  separation is constant ( $y = y_0$ ). (a) For  $y_0 = 0$ , the  $x$  separation increases monotonically. (b) For  $y_0 \neq 0$ , the  $x$  separation moves monotonically away from  $|y_0|$ , asymptotically approaching either zero or infinite  $x$  separation.

$$|x| \rightarrow \begin{cases} \left( \frac{2\mu b^2 t}{\pi \gamma (1 - \nu)} \right)^{1/2} & |x_0| > |y_0| \\ |x_0| e^{-\mu b^2 t / [\pi \gamma (1 - \nu) y_0^2]} & |x_0| < |y_0|. \end{cases} \quad (42)$$

In summary, in the zero-climb limit, the  $y$  separation (i.e., the separation perpendicular to the Burgers vectors  $\mathbf{b}_1 = \mathbf{b}_2$ ) remains constant, while the  $x$  separation (i.e., that parallel to the Burgers vectors) decreases if it is initially less than the  $y$  separation, or increases if it is initially greater than the  $y$  separation, asymptotically approaching either zero or infinite  $x$  separation, respectively.

We now return to Eqs. (36) and (37) and consider the case of finite climb (i.e., finite  $\Gamma$ ). For  $y = 0$ , we again have  $y = 0$ , and  $x(t)$  is again given by Eq. (39). Thus, we will restrict our attention to the case  $y_0 \neq 0$ . We first note that Eqs. (36) and (37) yield

$$\gamma x \dot{x} + \Gamma y \dot{y} = \frac{\mu b^2}{\pi (1 - \nu)}, \quad (43)$$

which is easily integrated to give

$$y = y_0 \left( 1 + \frac{2\mu b^2 t - \pi \gamma (1 - \nu) (x^2 - x_0^2)}{\pi \Gamma (1 - \nu) y_0^2} \right)^{1/2}. \quad (44)$$

Inserting Eq. (40) into Eq. (44) yields the path  $y(x)$  to first order in  $\gamma/\Gamma \ll 1$ :

$$y = y_0 \left\{ 1 + \frac{\gamma}{\Gamma} \left[ 2 \ln \left( \frac{x^2 - y_0^2}{x_0^2 - y_0^2} \right) - \ln \left( \frac{x}{x_0} \right) \right] \right\}, \quad (45)$$

which shows how  $y$  deviates from  $y_0$  near the stagnation loci  $y = \pm x$  and near the asymptotic values  $x = 0, \pm \infty$ . Note that this expression is valid only as long as the correction to  $y = y_0$  remains small, so that it breaks down too near the values  $x = 0, \pm y_0, \pm \infty$ .

To find the asymptotic behavior as  $t \rightarrow \infty$ , we cannot use Eq. (45) (since  $x \rightarrow 0, \pm \infty$ ), but, rather, we must return to Eqs. (36) and (37) (and we need not assume  $\Gamma \gg \gamma$ , but only  $\Gamma > \gamma$  for definiteness). For  $|x_0| < |y_0|$ , we have  $x \rightarrow 0$ , so that these equations become

$$\dot{x} = -\frac{\mu b^2 x}{\pi \gamma (1 - \nu) y^2}, \quad (46)$$

$$\dot{y} = \frac{\mu b^2}{\pi \Gamma (1 - \nu) y}. \quad (47)$$

The second equation yields

$$|y| \rightarrow \left( \frac{2\mu b^2 t}{\pi \Gamma (1 - \nu)} \right)^{1/2}, \quad (48)$$

and inserting this into the first equation gives

$$|x| \propto t^{-\Gamma/2\gamma}. \quad (49)$$

Finally, combining these results yields

$$|y| \propto |x|^{-\Gamma/\gamma}. \quad (50)$$

( $x$  and  $y$  always have the same signs as  $x_0$  and  $y_0$ , respectively). Thus, as  $t \rightarrow \infty$ , we have  $x \rightarrow 0$ , and  $|y| \rightarrow \infty$  along the path (50). Also, note that, for zero climb,  $x \rightarrow 0$  exponentially with time as Eq. (42), while, for finite climb,  $x \rightarrow 0$  as the power law (49).

Finally, for  $|x_0| > |y_0|$ , we have  $|x| \rightarrow \infty$  as  $t \rightarrow \infty$ , so that Eqs. (36) and (37) become

$$\dot{x} = \frac{\mu b^2}{\pi\gamma(1-\nu)x}, \quad (51)$$

$$\dot{y} = \frac{3\mu b^2 y}{\pi\Gamma(1-\nu)x^2}. \quad (52)$$

The first equation yields

$$|x| \rightarrow \left( \frac{2\mu b^2 t}{\pi\gamma(1-\nu)} \right)^{1/2}, \quad (53)$$

and inserting this into the second equation gives

$$|y| \propto t^{3\gamma/2\Gamma} \quad (54)$$

$$\propto |x|^{3\gamma/\Gamma}. \quad (55)$$

In summary, the trajectories are as shown in Fig. 3 (in this figure, we take  $x_0, y_0 > 0$ ; the other three cases are obtained by reflecting this figure through the  $x$  and/or  $y$  axes). For the trajectory with  $x \rightarrow 0$ , if  $\Gamma \gg \gamma$ , this trajectory crosses over from horizontal to vertical motion (i.e., the effects of finite  $\gamma/\Gamma$  become important) when  $|x| \approx \gamma |y_0|/\Gamma$ .

### V. ANTIPARALLEL BURGERS VECTORS ( $\alpha = \pi$ )

For  $\alpha = \pi$ , the overdamped equations of motion (34) and (35) become

$$\dot{x} = -\frac{\mu b^2 x(x^2 - y^2)}{\pi\gamma(1-\nu)(x^2 + y^2)^2} + \frac{2F_{xy}}{\gamma}, \quad (56)$$

$$\dot{y} = -\frac{\mu b^2 y(3x^2 + y^2)}{\pi\Gamma(1-\nu)(x^2 + y^2)^2} - \frac{2F_{xx}}{\Gamma}. \quad (57)$$

In order to obtain analytic solutions, we restrict our attention to the case with no external stress ( $F_{xy} = F_{xx} = 0$ ). In this case, these equations become the same as Eqs. (36) and (37) with  $\mu$  replaced by  $-\mu$ , and they are solved in exactly the same manner.

In the zero-climb limit,  $y$  is again constant ( $y = y_0$ ). For  $y_0 = 0$ , we have

$$x = x_0 \left( 1 - \frac{2\mu b^2 t}{\pi\gamma(1-\nu)x_0^2} \right)^{1/2}, \quad (58)$$

which shows that  $x$  moves monotonically toward  $x = 0$ , and the two dislocations meet and annihilate after a capture time

$$\tau_0 = \frac{\pi\gamma(1-\nu)x_0^2}{2\mu b^2}. \quad (59)$$

On the other hand, for  $y_0 \neq 0$ , we have

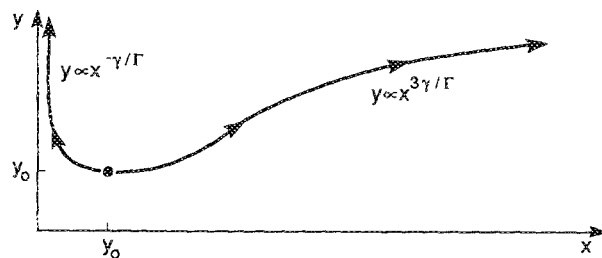


FIG. 3. Trajectories for parallel Burgers vectors ( $\alpha = 0$ ) in the overdamped limit ( $m^* \rightarrow 0$ ) with finite climb ( $\Gamma > \gamma$ ). For  $x_0 < 0$  and/or  $y_0 < 0$ , reflect this figure through the  $x$  and/or  $y$  axes, respectively.

$$t = \frac{\pi\gamma(1-\nu)}{2\mu b^2} \left[ x_0^2 - x^2 + 2y_0^2 \ln\left(\frac{x}{x_0}\right) - 4y_0^2 \ln\left(\frac{x^2 - y_0^2}{x_0^2 - y_0^2}\right) \right], \quad (60)$$

and  $x$  moves monotonically toward the nearer of the two points  $x = \pm y_0$  (see Fig. 4), approaching it asymptotically as

$$|x| = |y_0| \left[ 1 + \frac{1}{2} \left( \frac{x_0^2}{y_0^2} - 1 \right) e^{-\mu b^2 t / [2\pi\gamma(1-\nu)y_0^2]} \right]. \quad (61)$$

For finite climb, if  $y_0 = 0$ , we again have  $y = 0$ , and  $x(t)$  is again given by Eq. (58) with the capture time (59). For  $y_0 \neq 0$ , Eqs. (56) and (57) give (with no external stress)

$$\gamma x \dot{x} + \Gamma y \dot{y} = -\frac{\mu b^2}{\pi(1-\nu)}, \quad (62)$$

which yields

$$\gamma x^2 + \Gamma y^2 = \frac{2\mu b^2(\tau - t)}{\pi(1-\nu)}, \quad (63)$$

where  $\tau$  is the capture time

$$\tau = \frac{\pi(1-\nu)(\gamma x_0^2 + \Gamma y_0^2)}{2\mu b^2} \quad (64)$$

[notice that this reduces to Eq. (59) for  $y_0 = 0$ ]. Thus, for finite climb, in the absence of external stress, two antiparallel dislocations always meet and annihilate after the finite capture time (64).

For slow climb ( $\Gamma \gg \gamma$ ), we may again find how the trajectory begins to deviate from the line  $y = y_0$ . From Eqs. (63) and (64), we have

$$y = y_0 \left( 1 - \frac{2\mu b^2 t + \pi\gamma(1-\nu)(x^2 - x_0^2)}{\pi\Gamma(1-\nu)y_0^2} \right)^{1/2}, \quad (65)$$

and inserting Eq. (60) gives (to first order in  $\gamma/\Gamma$ )

$$y = y_0 \left\{ 1 - \frac{\gamma}{\Gamma} \left[ \ln\left(\frac{x}{x_0}\right) - 2 \ln\left(\frac{x^2 - y_0^2}{x_0^2 - y_0^2}\right) \right] \right\}. \quad (66)$$

This equation is valid as long as the correction to  $y = y_0$  remains small.

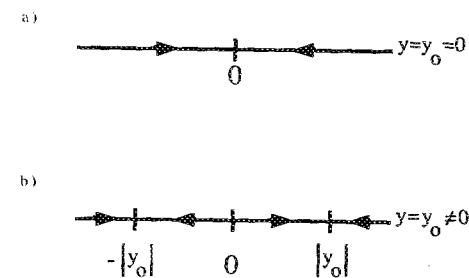


FIG. 4. For antiparallel Burgers vectors ( $\alpha = \pi$ ) in the overdamped limit ( $m^* \rightarrow 0$ ) with zero climb ( $\Gamma \rightarrow \infty$ ) and no external stress ( $F_{xy} = F_{xx} = 0$ ), the  $y$  separation is constant ( $y = y_0$ ), while the  $x$  separation monotonically approaches the  $y$  separation ( $x \rightarrow \pm y_0$ ). (a) For  $y_0 = 0$ , the two dislocations meet and annihilate after a finite capture time  $\tau_0 = \pi\gamma(1-\nu)x_0^2/2\mu b^2$ , while (b) for  $y_0 \neq 0$ , the approach  $x \rightarrow \pm y_0$  is only asymptotic as  $t \rightarrow \infty$ .

For finite climb ( $\Gamma > \gamma$ ), Eq. (63) shows that  $x, y \rightarrow 0$  as  $t \rightarrow \tau$ . To find this asymptotic behavior, we return to Eqs. (56) and (57) (with  $F_{xy} = F_{xx} = 0$ ). Since  $x \rightarrow 0$ , Eq. (56) requires that  $|y| \ll |x|$  asymptotically. Thus, as  $t \rightarrow \tau$ , the origin is approached with a slope  $\lambda$  satisfying  $0 < |\lambda| \ll 1$ , and we will consider the two cases  $\lambda = 0$  and  $\lambda \neq 0$  separately. For  $\lambda = 0$ , we have the asymptotic result  $|y| \ll |x|$ , and Eqs. (56) and (57) become

$$\dot{x} = -\frac{\mu b^2}{\pi \gamma (1-\nu)x}, \quad (67)$$

$$\dot{y} = -\frac{3\mu b^2 y}{\pi \Gamma (1-\nu)x^2}. \quad (68)$$

The first equation yields

$$|x| \rightarrow \left( \frac{2\mu b^2 (\tau - t)}{\pi \gamma (1-\nu)} \right)^{1/2}, \quad (69)$$

and inserting this into the second equation gives

$$|y| \propto (\tau - t)^{3/2\Gamma} \quad (70)$$

$$\propto |x|^{3\gamma/\Gamma}. \quad (71)$$

Note that this solution is valid only for  $\Gamma < 3\gamma$ , since we assumed the origin was approached with zero slope.

For finite slope  $\lambda \neq 0$ , we have the asymptotic behavior

$$y = \lambda x, \quad (72)$$

and Eqs. (56) and (57) become

$$\dot{x} = -\frac{\mu b^2 (1 - \lambda^2)}{\pi \gamma (1-\nu) (1 + \lambda^2)^2 x}, \quad (73)$$

$$\dot{y} = \lambda \dot{x} = -\frac{\mu b^2 \lambda (3 + \lambda^2)}{\pi \Gamma (1-\nu) (1 + \lambda^2)^2 x}. \quad (74)$$

Combining these two equations yields the magnitude of the slope:

$$|\lambda| = \left( \frac{\Gamma - 3\gamma}{\Gamma + \gamma} \right)^{1/2}, \quad (75)$$

so that this solution is valid only for  $\Gamma > 3\gamma$ . For this value of  $|\lambda|$ , Eqs. (73) and (74) become the single equation

$$\dot{x} = -\frac{\mu b^2 (\Gamma + \gamma)}{\pi (1-\nu) (\Gamma - \gamma)^2 x}. \quad (76)$$

Equation (76) yields

$$|x| \rightarrow \left( \frac{2\mu b^2 (\Gamma + \gamma) (\tau - t)}{\pi (1-\nu) (\Gamma - \gamma)^2} \right)^{1/2}, \quad (77)$$

and inserting this into Eq. (72) gives [using Eq. (75)]

$$|y| \rightarrow \left( \frac{\Gamma - 3\gamma}{\Gamma + \gamma} \right)^{1/2} |x| \quad (78)$$

$$\rightarrow \left( \frac{2\mu b^2 (\Gamma - 3\gamma) (\tau - t)}{\pi (1-\nu) (\Gamma - \gamma)^2} \right)^{1/2}. \quad (79)$$

In summary, for  $\Gamma < 3\gamma$ , we have the asymptotic behavior (69)–(71), and, for  $\Gamma > 3\gamma$ , we have the asymptotic behavior (77)–(79). Since we typically have  $\Gamma \gg \gamma$ , it is the latter case which is expected to occur, and these results are shown in Fig. 5. For slow climb ( $\Gamma \gg \gamma$ ), the motion stays close to the two dashed lines: the  $x$  separation quickly adjusts to the nearly constant  $y$  separation in a time  $\tau_0 = \pi \gamma (1-\nu) x_0^2 / 2\mu b^2$ , after which the two dislocations

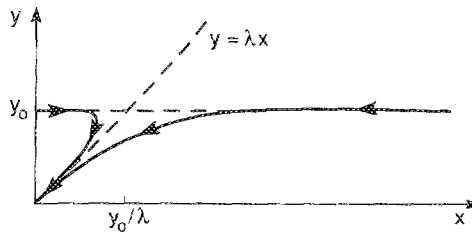


FIG. 5. Trajectories for antiparallel Burgers vectors ( $\alpha = \pi$ ) in the overdamped limit ( $m^* \rightarrow 0$ ) with finite climb ( $\Gamma > 3\gamma$ ) and no external stress ( $F_{xy} = F_{xx} = 0$ ). Here,  $\lambda = [(\Gamma - 3\gamma)/(\Gamma + \gamma)]^{1/2}$ . For slow climb ( $\Gamma \gg \gamma$ ), the motion stays very close to the two dashed lines. For  $x_0 < 0$  and/or  $y_0 < 0$ , reflect this figure through the  $x$  and/or  $y$  axes, respectively.

slowly approach along the line  $y = \lambda x$ , annihilating after an additional time  $\tau - \tau_0 = \pi \Gamma (1-\nu) y_0^2 / 2\mu b^2$ . When the climb is less slow, this transition is less sharp (as shown in Fig. 5).

## VI. PERPENDICULAR BURGERS VECTORS ( $\alpha = \pi/2$ )

For  $\alpha = \pi/2$ , the overdamped equations of motion (34) and (35) become

$$\dot{x} = \left( \frac{1}{\gamma} + \frac{1}{\Gamma} \right) \frac{\mu b^2 y (x^2 - y^2)}{2\pi (1-\nu) (x^2 + y^2)^2} + \frac{F_{xy}}{\gamma} - \frac{F_{yy}}{\Gamma}, \quad (80)$$

$$\dot{y} = -\left( \frac{1}{\gamma} + \frac{1}{\Gamma} \right) \frac{\mu b^2 x (x^2 - y^2)}{2\pi (1-\nu) (x^2 + y^2)^2} + \frac{F_{xy}}{\gamma} - \frac{F_{xx}}{\Gamma}. \quad (81)$$

In this case, there is no advantage in taking the limit of zero climb ( $\Gamma \rightarrow \infty$ ), or even slow climb ( $\Gamma \gg \gamma$ ), so we immediately consider the case of finite climb ( $\Gamma > \gamma$ ).

We again restrict our attention to the case with no external stress ( $F_{xy} = F_{xx} = F_{yy} = 0$ ). Equations (80) and (81) then yield

$$x\dot{x} + y\dot{y} = 0, \quad (82)$$

which is easily integrated to give

$$x^2 + y^2 = r_0^2 = x_0^2 + y_0^2, \quad (83)$$

showing that the relative motion is constrained to the circle  $r = r_0 = r(0)$  (i.e., the distance between the two dislocations remains constant). In particular, the two dislocations can neither meet nor escape to infinite separation. From Eqs. (80) and (81), we see that the stagnation loci are again the lines  $y = \pm x$  (since this is where  $\dot{x} = \dot{y} = 0$ ), which divide the circle  $r = r_0$  into four arcs (see Fig. 6), with the motion being confined to one of these arcs.

Since the relative motion is confined to the circle  $r = r_0$ , it is convenient to switch to polar coordinates:

$$x = r_0 \cos \theta, \quad (84)$$

$$y = r_0 \sin \theta, \quad (85)$$

in which case, Eqs. (80) and (81) reduce to the single equation (in the absence of external stress)

$$\dot{\theta} = -\frac{\mu b^2}{2\pi(1-\nu)r_0^2} \left( \frac{1}{\gamma} + \frac{1}{\Gamma} \right) \cos 2\theta, \quad (86)$$

which is easily integrated to yield

$$\theta = \theta_\infty + \arctan \left[ e^{-\mu b^2(\gamma^{-1} + \Gamma^{-1})/[\pi(1-\nu)r_0^2]} \times \tan(\theta_0 - \theta_\infty) \right], \quad (87)$$

where  $\theta_0 = \theta(0)$  and  $\theta_\infty = -\frac{1}{4}\pi$  or  $\frac{3}{4}\pi$ , whichever is nearer to  $\theta_0$ . Thus, we see that  $\theta$  moves monotonically toward the nearer of the two angles  $\theta_\infty = -\frac{1}{4}\pi, \frac{3}{4}\pi$  (i.e., the motion is along the circle  $r = r_0$ , toward the nearer of the two points where this circle intersects the line  $y = -x$ , as shown in Fig. 6). Furthermore, as  $t \rightarrow \infty$ , we have the asymptotic behavior

$$\theta \rightarrow \theta_\infty + e^{-\mu b^2(\gamma^{-1} + \Gamma^{-1})/[\pi(1-\nu)r_0^2]} \tan(\theta_0 - \theta_\infty), \quad (88)$$

showing an exponentially slowing approach to the limiting value  $\theta_\infty$ .

In Sec. III, we found the motion of the center of mass only for the cases of parallel ( $\alpha = 0$ ) and antiparallel ( $\alpha = \pi$ ) Burgers vectors, and we stated that, for  $\alpha \neq 0, \pi$ , the center-of-mass motion is very complicated. This is fairly easy to demonstrate for perpendicular Burgers vectors ( $\alpha = \pi/2$ ). In the zero-climb limit ( $\Gamma \rightarrow \infty$ ), Eqs. (13) and (15) become (since  $\eta_2 = -x_2$ )

$$\dot{y}_1 = 0, \quad (89)$$

$$\dot{x}_2 = 0, \quad (90)$$

which yield  $y_1 = y_{10} = y_1(0)$  and  $x_2 = x_{20} = x_2(0)$ . Thus, the center-of-mass coordinates are given by

$$X = \frac{1}{2}(x_1 + x_2) = x_2 + \frac{1}{2}(x_1 - x_2) = x_{20} + \frac{1}{2}x, \quad (91)$$

$$Y = \frac{1}{2}(y_1 + y_2) = y_1 - \frac{1}{2}(y_1 - y_2) = y_{10} - \frac{1}{2}y, \quad (92)$$

showing that, even in the zero-climb limit, the center-of-mass motion is as complicated as the relative motion (for finite climb, it is even more complicated).

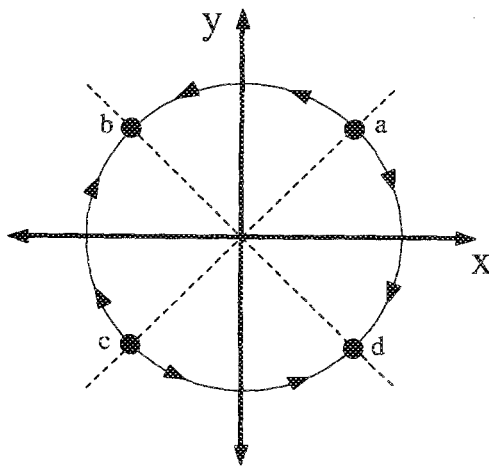


FIG. 6. Trajectories for perpendicular Burgers vectors ( $\alpha = \pi/2$ ) in the overdamped limit ( $m^* \rightarrow 0$ ) with finite climb ( $\Gamma > \gamma$ ) and no external stress ( $F_{xy} = F_{yx} = F_{yy} = 0$ ). The distance between the two dislocations remains constant, so that the relative motion is along a circle. Furthermore, the motion is along one of the four arcs between the stagnation points a, b, c, and d, moving monotonically away from a or c and toward b or d.

## VII. MOTION FOR $\alpha \neq 0, \pi/2, \pi$

Except for the three special cases  $\alpha = 0, \pi/2, \pi$  examined in Secs. IV–VI, we cannot find analytic expressions for the relative motion  $\mathbf{r}(t)$ . For these three special cases, a common thread is the existence of stagnation loci (points where  $\dot{x} = \dot{y} = 0$ ) which either attract or repel the motion. However, for  $\alpha \neq 0, \pi/2, \pi$ , no such stagnation loci exist (other than zero or infinite separation). In particular, this means that, for these other cases, the two dislocations either meet or separate to infinity as  $t \rightarrow \infty$ . To see this, we return to the equations of motion (12)–(15). In the overdamped limit ( $m^* \rightarrow 0$ ) with zero climb ( $\Gamma \rightarrow \infty$ ) and no external stress ( $F_{ij} = 0$ ), these equations again become Eqs. (16)–(19):

$$\gamma \dot{x}_1 = \frac{\mu b^2}{2\pi(1-\nu)r} \cos 2\theta \cos(\theta - \alpha), \quad (93)$$

$$\gamma \dot{\xi}_2 = -\frac{\mu b^2}{2\pi(1-\nu)r} \cos \theta \cos 2(\theta - \alpha), \quad (94)$$

$$\dot{y}_1 = 0, \quad (95)$$

$$\dot{\eta}_2 = 0. \quad (96)$$

Since the relative coordinates are

$$x = x_1 - x_2 = x_1 - \xi_2 \cos \alpha + \eta_2 \sin \alpha, \quad (97)$$

$$y = y_1 - y_2 = y_1 - \xi_2 \sin \alpha - \eta_2 \cos \alpha, \quad (98)$$

then, if we exclude the cases  $\alpha = 0, \pi$ , the requirements  $\dot{x} = \dot{y} = 0$  for stagnation points are equivalent to the conditions  $\dot{x}_1 = \dot{\xi}_2 = 0$ , which yield

$$\cos 2\theta \cos(\theta - \alpha) = 0, \quad (99)$$

$$\cos \theta \cos 2(\theta - \alpha) = 0. \quad (100)$$

Multiplying the first equation by  $\sin(\theta - \alpha)$  and the second by  $\sin \theta$  and subtracting the results yields the requirement (after some algebra)

$$\sin 2\alpha = 0, \quad (101)$$

which shows that stagnation points are impossible unless  $\alpha = 0, \pi/2, \pi$  (remember that the labels are chosen so as to make  $0 < \alpha < \pi$ ). This absence of stagnation loci for  $\alpha \neq 0, \pi/2, \pi$  implies that, when such dislocation orientations exist, the motion is qualitatively different than for the special cases considered in Secs. IV–VI.

## VIII. SUMMARY

We have analyzed in detail the relative motion of a pair of edge dislocations with parallel line directions due to their mutual interactions in the overdamped limit ( $m^* \rightarrow 0$ ). We have obtained analytic results for the trajectories in the three cases of parallel, antiparallel, and perpendicular Burgers vectors for both zero climb and finite climb. In each case, there are “stagnation” points (stable or unstable equilibria), which are either attracting or repelling, and these stagnation points allow a simple characterization of the motion. In addition, we have shown that, for all other orientations of the two Burgers vectors, no such stagnation points exist. In such cases, the pair of dislocations must eventually come together or separate to infinity.

When an external stress is applied, the same approach can be used, but the resulting expressions for the trajectories

are too complicated to be of practical use. In this case, we have instead given the first-order equations of motion for the trajectories, which may simply be solved numerically.

#### ACKNOWLEDGMENT

D.J.S. acknowledges the support of the U.S. Department of Energy, Grant No. DE-FG02-88ER45367.

<sup>1</sup>R. Eykholt, S. A. Trugman, and D. J. Srolovitz, *J. Appl. Phys.* **65**, 4198 (1989).

<sup>2</sup>J. Lepinoux and L. P. Kubin, *Scr. Metall.* **21**, 833 (1987).

<sup>3</sup>N. M. Ghonhiem and R. Amodeo, in *Nonlinear Phenomena in Materials Science*, edited by G. Martin and L. P. Kubin (Transtech, Aedermannsdorf, Switzerland, 1988).

<sup>4</sup>A. Gulluoglu, D. J. Srolovitz, and P. S. Lomdahl (unpublished).

<sup>5</sup>J. Weertman, in *Response of Metals to High Velocity Deformation*, edited by P. G. Shewmon and V. F. Zackay (Interscience, New York, 1961), p. 205.

<sup>6</sup>R. W. Lardner, *Mathematical Theory of Dislocations and Fracture* (University of Toronto Press, Toronto, 1974), Chap. 3.

<sup>7</sup>M. Peach and J. S. Koehler, *Phys. Rev.* **80**, 436 (1950).

<sup>8</sup>J. P. Hirth and J. Lothe, *Theory of Dislocations* (McGraw-Hill, New York, 1982), Chaps. 7 and 15.